Pairing-plus-quadrupole model calculations for ^{154,156}Gd†

J. B. Gupta
Ramjas College, University of Delhi, Delhi, India

Krishna Kumar and J. H. Hamilton
Physics Department,† Vanderbilt University, Nashville, Tennessee 37235

(Received 22 February 1977)

The question of validity of the pairing-plus-quadrupole model to well-deformed nuclei is examined. The calculated energy levels, $B(E2)$ values, $E2/M1$ mixing ratios, and electromagnetic moments are compared with the experimental values of ^{156}Gd which is used as a test case. In particular, the structure of the second excited $K = 0$ band and the $K = 4$ band are examined in terms of model wave functions. For the sake of comparison and discussion, some results are also given for ^{154}Gd.

[NUCLEAR STRUCTURE ^{156}Gd—calculated level energies, $B(E2)$ values, quadrupole moments, magnetic moments, $E2$ and $M1$ matrix elements, $\delta(E2/M1)$, β_{rms}, γ_{rms}. ^{154}Gd—calculated $B(E2)$ values. Comparison with experiment whenever possible.]

I. INTRODUCTION

The rotational model of Bohr and Mottelson[1] provides an excellent starting point for analyzing and studying nuclear spectra. However, the model including small amplitude vibrations fails to explain the decay characteristics of low energy levels in rare-earth nuclei (see, e.g., the review by Hamilton[2]). This is especially true for the β-vibrational band. Furthermore, the second $K^\pi = 0^+$ vibrational bands observed in these nuclei have characteristics different from those of the first 0^+- (or β-) vibrational bands which are not understood in terms of the phenomenological models. A microscopic treatment of the problem is considered necessary for gaining more insight into the structure of these nuclei.

The pairing-plus-quadrupole model in the time-dependent–Hartree-Bogolyubov picture developed by Kumar and Baranger[3,4] has provided a deeper understanding of the shape transitions from prolate to oblate[3] and spherical to deformed[4] around the $A = 150$ and 200 regions. These studies have provided a detailed understanding of the decay characteristics of the β-vibrational and γ-vibrational bands in the transitional nuclei of this region.

It was proposed to test the applicability of this microscopic approach to somewhat more deformed nuclei. The spectra of the Gd nuclei present a good opportunity for such a test since these nuclei span the region from nearly spherical to well-deformed nuclei. As one moves through the even-even Gd nuclei, the β, γ, and the second 0^+ bands cross in energy. While the β and γ bands cross each other in ^{154}Gd, the second 0^+ band also comes down quite low in ^{156}Gd. Yet, the 0^+ bands mix very little.[5] Thus, these nuclei provide some of the most interesting cases for testing the microscopic theory mentioned above.

Some preliminary results of such a study were presented earlier.[6] Detailed results for ^{156}Gd are presented below along with some results for ^{154}Gd. Detailed results for ^{154}Gd will be presented in a subsequent publication.

The microscopic theory is reviewed briefly in Sec. II. Our choice of theoretical parameters, the calculated results, and comparison with experiment are discussed in Sec. III. Summary and conclusions are given in Sec. IV.

II. THEORY

A detailed account of the Kumar-Baranger method of treating the pairing-plus-quadrupole model can be found in the recent review by Kumar.[7] Salient points of the theory are repeated here briefly for reference.

An ideal microscopic theory of collective motion differs from a phenomenological collective model in that the parameters of the collective Hamiltonian are derived from a microscopic theory, instead of being taken from experiment. The Kumar-Baranger theory is a semimicroscopic (or semiphenomenological) one since although the potential and kinetic energies of collective motion are calculated via some lengthy integrals over the nucleon coordinates, the calculated energies have to be renormalized via two parameters (see Sec. III). However, the number of these parameters is much smaller than that required in a purely phenomenological approach.

In the Kumar-Baranger theory, one starts from

a spherical-shell model Hamiltonian (an oscillator potential including $\vec{l}\cdot\vec{s}$ and $\vec{l}^2$ terms) and takes into account the two most important residual-two-body interactions coming from the long range quadrupole force and the short range pairing force. Thus, the pairing-plus-quadrupole model Hamiltonian is written as

$$H_{\mathrm{PPQ}} = H_{\mathrm{SS}} + H_Q + H_P \,, \tag{1}$$

where H_{SS} is the spherical-shell Hamiltonian; H_Q is a $Q\cdot Q$ interaction with $J=2$, $T=0$; and H_P is a pair-pair interaction with $J=0$, $T=1$.

The eigenvalues of H_{SS}, the spherical single-particle (s.p.) energies, are the input parameters of the theory (same values are used for a certain region except for an overall A-dependent factor). The calculation is limited to the two outermost oscillator shells, two for neutrons and two for protons. Effects of the nuclear core are taken into account via a renormalization method.[4]

The PPQ Hamiltonian of Eq. (1) is solved via a time-dependent–Hartree-Bogolyubov method. This leads to three main steps of the calculation.

(i) A Nilsson transformation is performed from the spherical s.p. basis to a deformed s.p. basis. A quadrupole deformation potential depending on the nuclear shape variables β and γ is added to H_{SS}, and the resulting Hamiltonian is diagonalized in the spherical basis to obtain the level energies η_i and the eigenvectors $\langle nljm\,|\,i\rangle$. Two calculations are performed, one for protons and one for neutrons, for each set of β and γ.

(ii) A Bogolyubov-Valatin transformation is performed from the deformed s.p. basis to a deformed quasiparticle basis. For each (β,γ) set, two BCS calculations are performed to get the energy gaps (Δ) and the u and v factors for protons and for neutrons. Strengths of the pairing force, G_p and G_n are taken from previous fits to odd-even mass differences.[3,4]

The expectation value of H_{PPQ} with respect to the deformed–zero-quasiparticle state (often called a BCS state) gives the potential energy of deformation, $V(\beta,\gamma)$.

A second order, time-dependent perturbation due to the dynamics of collective nuclear motion gives corrections to the energy calculated as described above. These corrections are identified as the kinetic energy of collective motion and the total energy is expressed as a semiclassical, collective Hamiltonian

$$H_C = V(\beta,\gamma) + T_{\mathrm{rot}} + T_{\mathrm{vib}} \,, \tag{2}$$

where

$$T_{\mathrm{rot}} = \frac{1}{2}\sum_{k=1}^{3} \mathcal{I}_k \omega_k^2 \,, \tag{3}$$

and

$$T_{\mathrm{vib}} = \tfrac{1}{2}B_{\beta\beta}(\beta,\gamma)\dot{\beta}^2 + B_{\beta\gamma}\,\beta\dot{\beta}\dot{\gamma} + \tfrac{1}{2}B_{\gamma\gamma}(\beta,\gamma)\beta^2\dot{\gamma}^2 \,. \tag{4}$$

Expressions for the three rotational moments of inertia $\mathcal{I}_k$ and the three vibrational mass parameters $B_{\beta\beta}$, $B_{\beta\gamma}$, and $B_{\gamma\gamma}$ have been given previously.[7] In addition to these six kinetic functions and the potential function mentioned above, we calculate microscopically the expectation values of six operators needed for determining the electromagnetic moments, transition probabilities, and the mixing ratios. These six operators consist of one monopole operator (r^2), two quadrupole operators (Q_{20}, Q_{22}), and three gyromagnetic ratio operators (g_k).

All 13 functions are computed for each point of a β-γ mesh consisting of 92 points.

(iii) The collective Schrödinger equation, depending on the quantized form of the Hamiltonian of Eqs. (2)–(4), is solved via numerical methods[7] in the basis

$$\Psi_{\alpha IM} = \sum_K A_{\alpha IK}(\beta,\gamma)\Phi^I_{MK}(\phi,\theta,\Psi) \,, \tag{5}$$

where I is total angular momentum of the nucleus; M and K are the projections of $\vec{I}$ on the lab-z axis and intrinsic-z axis; $\alpha = 1, 2, \ldots,$ denotes the first second, ..., level (in order of increasing energy) with the same I; Φ^I_{MK} is a symmetrized sum of the D functions depending on the Euler angles ϕ, θ, and Ψ. Since the functions Φ^I_{MK} are known (they can be viewed as generalized spherical harmonics), the numerical method mentioned above yields the "vibrational" wave functions $A_{\alpha IK}$. Note that because of symmetry conditions, we have $K = 0, 2, \ldots, I$ for I = even and $K = 2, 4, \ldots, (I-1)$ for I = odd.

III. CHOICE OF PARAMETERS AND RESULTS

A. Parameters

As pointed out above, since only two harmonic oscillator shells are used for protons and neutrons, corrections have to be made for the nuclear core contributions. An improved method of including these corrections, as discussed by Kumar,[4] is employed here. All the calculated kinetic functions are multiplied by an inertial renormalization factor F_B. The potential function depends on one fitting parameter, the quadrupole force strength χ. These two parameters are determined by fitting the experimental energies of the lowest 2^+ and 4^+ states.

The two parameters are somewhat interdependent and are not determined uniquely. We make a

compromise by first varying χ so as to fit the ratio E_4/E_2, and then varying F_B so as to fit the absolute values of the excitation energies. In so doing, we obtained $\chi = 68A^{-1.4}$ MeV, $F_B = 2.3$ for ^{156}Gd; and $\chi = 70A^{-1.4}$ MeV, $F_B = 2.4$ for ^{154}Gd. The corresponding values were 70 and 2.8 for[4] ^{152}Sm.

The two-dimensional collective wave functions, $A_{\alpha IK}$ of Eq. (5), are expanded[7] in a basis of analytic functions depending on two range parameters b_x and b_y. These two range parameters are determined by minimizing the ground state energy.

The effective charge parameter is taken from a previous fit to the known $B(E2; 0 \rightarrow 2)$ value for ^{152}Sm.

B. Level energies

Energies of the calculated levels ($\pi = +$) of ^{156}Gd are given in Table I. Grouping of the calculated levels into the five bands is based on the largest K component of the calculated wave functions, and on the decay characteristics of the levels.

Comparison with experiment[8,9] shows that the energy of the 6^+ state of the ground state band (6_g) is reproduced within 2%. The β- and γ-vibrational bandheads are higher by 0.18 and 0.38 MeV, respectively. The γ-band spread is given correctly, but the β-band spread is slightly larger. Energy of the second 0^+ vibrational bandhead, and the bandspread, are higher by a factor of 2. The $K^\pi = 4^+$ bandhead lies at about twice the experimental energy, but the band spread is reproduced correctly. It is, of course, possible that the experimental second 0^+ and $K^\pi = 4^+$ bands are not of the same origin as those calculated.

TABLE I. Level energies, β_{rms}, γ_{rms}, quadrupole moments (QM), and magnetic moments (MM) for ^{156}Gd.

Level I	Energy (MeV) Expt.[a]	Energy (MeV) Theo.	Present theory β_{rms}	Present theory γ_{rms}	Present theory QM (e b)	Present theory MM (μ_N)
			g band			
0	0.0	0.0	0.273	12.9	0.0	0.0
2	0.089	0.087	0.276	12.8	−1.88	0.82
4	0.288	0.283	0.281	12.4	−2.42	1.63
6	0.585	0.569	0.287	12.1	−2.68	2.44
			β band			
0	1.049	1.234	0.281	9.6	0.0	0.0
2	1.129	1.419	0.301	9.2	−1.78	0.78
4	1.298	1.618	0.301	10.3	−2.19	1.56
6		1.887				
			γ band			
2	1.154	1.531	0.275	19.8	1.65	0.79
3	1.248	1.606	0.277	18.2	0.0	1.21
4	1.355	1.762	0.283	19.6	−1.17	1.62
5	1.507	1.874	0.282	19.0	−1.46	2.04
			0^+ band			
0	1.168	2.275	0.300	3.4	0.0	0.0
2	1.258	2.586	0.289	5.1	−1.68	0.79
4	1.462	2.833	0.323	8.2	−2.04	1.55
			4^+ band			
4	1.511	2.989	0.282	22.4	2.66	1.57
5	1.623	3.095	0.301	18.7	0.02	1.98

[a] See Refs. 8 and 9.

C. β_{rms}, γ_{rms}, quadrupole and magnetic moments

Values of these four quantities include the effects of the dynamics of nuclear motion since they are obtained by summing the matrix elements of the appropriate operators over all points of the β-γ mesh.

Table I shows that while the β_{rms} values are remarkable in their similarity (variation over different members of all five bands is $< 20\%$), the γ_{rms} values show much more variation (3° to 22°). Comparison with a similar calculation for ^{150,152}Sm (Tables 1 and 2 of Ref. 4) shows that the increase of β_{rms} with I becomes slower as one moves towards the middle of the deformed region. Thus, in the case of excitation from the g.s. to the first 2^+ state, there is a 13% increase in β_{rms} in ^{150}Sm, 3% in ^{152}Sm, but only 1% in ^{156}Gd. The corresponding increase in β_{rms} for excitation to the O_β state is 13% for ^{150}Sm, 10% for ^{152}Sm, and 3% for ^{156}Gd. These results provide concrete justification for classifying ^{156}Gd as a well-deformed nucleus which is quite rigid against β vibrations or centrifugal stretching.

A similarly reduced variation in γ_{rms} is observed in ^{156}Gd both with rotation (increase of I within the same band) and with vibration. Effect of the centrifugal term proportional to $I_3^2/\mathcal{I}_3 \approx K^2/\gamma^2$ in increasing the average value of γ_{rms} with K is quite evident in Table I.

The spectroscopic quadrupole moments are given in the rotational model by

$$Q^S(I) = \frac{3K^2 - I(I+1)}{(I+1)(2I+3)} Q_0 , \tag{6}$$

where Q_0 is the intrinsic quadrupole moment. Variations in the magnitudes and signs of the calculated Q^S (see Table I) are given largely by Eq. (6). But the deduced Q_0 values increase slightly with spin for the g and γ bands, and decrease by about 5% for the β and 0^+ bands. Our calculated value for $Q(2_g)$ is in reasonable agreement with experiment[10] (see Table II).

The spectroscopic magnetic moments are given in the rotational model by

$$\mu^S_{\alpha I} = gI , \tag{7}$$

where g is the intrinsic gyromagnetic ratio, or the g value. From Table I, one sees that the calculated g values show <5% variation with rotation (I) as well as vibration (different bands).

This variation as well as the absolute values of the magnetic moments agrees well with experiment[10-12] for the $2^+, 4^+$ members of the g band (Table II). In the case of the 4^+ member of the $K^\pi = 4^+$ band, our value is smaller by a factor of 2. However, this disagreement is perhaps not surprising in view of the fact that Weitsch and Walter[11] called this state a two quasiparticle state with the structure $[411\uparrow]_p[413\downarrow]_p$.

D. Shape dependence of the potential function and the mass parameters

Figure 1 gives a contour plot of the potential function $V(\beta,\gamma)$, for ^{156}Gd. The equipotential curves have the $(\beta-\beta_0)^2$ variation expected for a well-deformed, axially symmetric nucleus of prolate shape at small values $(\beta-\beta_0)$. The asymmetry in the curves is partly due to the γ dependence of $V(\beta,\gamma)$ and partly due to higher order terms in $(\beta-\beta_0)$.

Plots of $V(\beta,\gamma)$ vs β for different fixed values of γ are shown in Fig. 2, where the calculated and the experimental levels are also plotted. The lowest potential minimum occurs for $\gamma=0°$ (prolate) at $\beta=0.27$, and is 4.5 MeV deep relative to the spherical maximum. Compare this with the value 1.2 and 3.1 MeV in ^{150}Sm and ^{152}Sm, respectively.[4] The calculated ground state (g.s.) of ^{156}Gd lies at 2.0 MeV above the potential minimum (i.e., the energy of zero-point motion is 2 MeV), which is

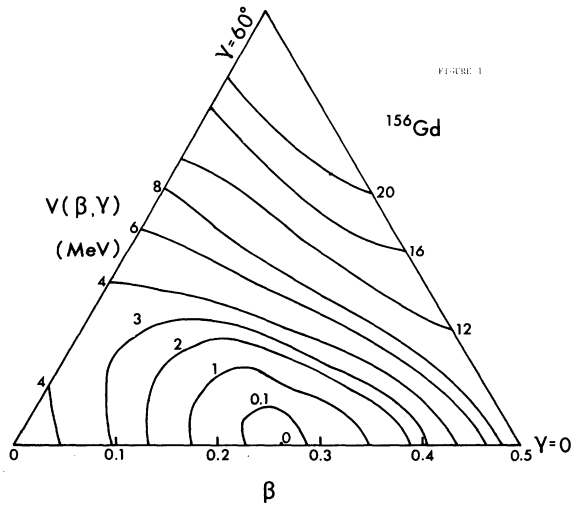

FIG. 1. Contour plot of the potential energy of ^{156}Gd. The lowest minimum occurs for a prolate shape ($\beta=0.27$ $\gamma=0°$).

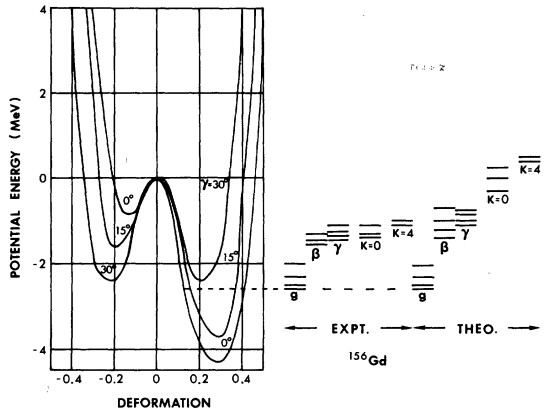

FIG. 2. Plots of V (β,γ=fixed) vs β and the energy levels of ^{156}Gd. Level energies are normalized to the calculated ground state energy (shown with a dashed line) which includes the energy of zero-point motion. Note that the potential minima for $\beta<0$ are not true minima but saddle points, being maxima in the γ direction.

2.5 MeV below the spherical barrier and 1.6 MeV below the oblate barrier (a saddle point, being a local minimum in β and a maximum in γ).

Of the calculated five bands, four lie below the spherical energy, further demonstrating ^{156}Gd to be a well-deformed nucleus. The calculated energies agree quite well with experiment except for the discrepancies noted above.

The β and γ dependences of the mass parameters [$B_{\beta\beta}, B_{\beta\gamma}$, and $B_{\gamma\gamma}$ of Eq. (4)] and the moments of inertia [$\mathcal{I}_1$, $\mathcal{I}_2$, and $\mathcal{I}_3$ of Eq. (3)] are quite different from those of V. They affect the collective motion in many important ways. For example, a sharp maximum in the mass parameters can produce a local wave function maximum even in β and γ regions where no potential minimum exists. The nucleus can lower its total energy not only via its potential energy but also via its kinetic energy. For the sake of abbreviation, we give only the contour plot of $B_{\beta\beta}(\beta,\gamma)$ in Fig. 3 (see Ref. 7 for more complete plots). But for the sake of discussion, we give below the main features of the β and γ variations of all three mass parameters.

The three mass parameters depend on β and γ quite differently. While $B_{\gamma\gamma}$ varies slowly, the function $B_{\beta\beta}$ varies by a factor of 5. Although the variation in $B_{\beta\beta}$ is small for $\beta<\beta_0$ ($\gamma<30°$), a steep minimum occurs at $\beta=0.3$, $\gamma=0°$ and the maximum value is obtained for an oblate ($\gamma=60°$) shape. As regards $B_{\beta\gamma}$, it is small near the prolate, oblate edges (since the symmetry conditions make it vanish along these edges[7]). But $B_{\beta\gamma}$ becomes as large as $B_{\beta\beta}$ and $B_{\gamma\gamma}$ at $\gamma\sim30°$ and $\beta>\beta_0$.

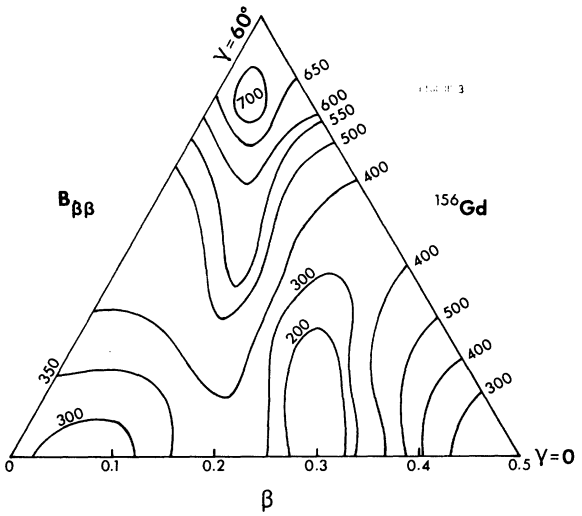

FIG. 3. Contour plot of the β-vibrational mass parameter of ^{156}Gd. This mass parameter is not simply a constant, independent of β and γ, as assumed in most theories of collective motion.

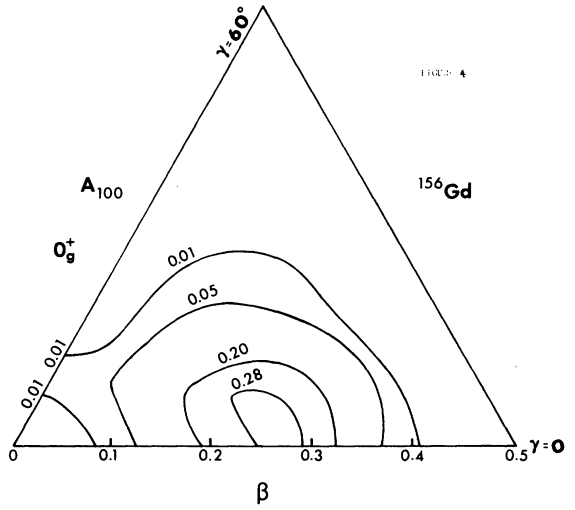

FIG. 4. Contour plot of the ground state wave function of ^{156}Gd. Although the maximum occurs near the potential minimum, the wave function is spread over a substantial portion of the β-γ plane.

E. K-β-γ dependence of the wave functions

The β and γ dependences of the vibrational part $A_{\alpha IK}$ of the nuclear wave function, defined in Eq. (5), are best seen in plots in the β-γ plane. For the sake of brevity, such plots are given only for the five bandheads in Figs. 4–8.

1. *g band ($K^\pi = 0^+$)*

The wave function A_{100} for the O_g state has a maximum on the prolate edge with slight asymmetry (see Fig. 4). The small value of the wave function at the far edge ($\beta = 0.5$) of the β-γ triangle illustrates the convergence obtained in the present numerical solution of the collective Hamiltonian. The plot of the 2_g, $K=0$ wave function A_{120} (not shown) is similar to the A_{100} plot. The A_{122} component contributes less than 5% to the normalization of the wave function.

2. *β band and second $K^\pi = 0^+$ band*

The β and γ dependences of the A_{200} and A_{300} wave functions (Figs. 5 and 6) for the 0^+ states are quite different, both being different from the g.s. There is a node close to the equilibrium deformation in A_{200}. There are two nodes in A_{300}. Comparison with a similarly deformed nucleus, ^{154}Sm (Ref. 13), shows that there is an admixture of prolate, oblate, and spherical shapes in the third 0^+ state as observed in the m band of ^{154}Sm, but there is more asymmetry in the present case. The A_{220} and A_{420} wave functions of the 2_β and 2_0^+ states are similar to A_{200} and A_{300}, respectively. Contribution of the $K=2$ component to the 2^+ states is 20 and 10%, respectively.

3. *γ band and $K^\pi = 4^+$ band*

The plot for A_{322} (Fig. 7), the $K=2$ component of the γ bandhead, shows that the wave function lies off the prolate edge because of γ vibrations. The $K=0$ component of this state is only 14%. The 3_γ and 5_γ state wave functions are quite similar to the $2_\gamma 2$ wave function (A_{322}), and also to the 4^+

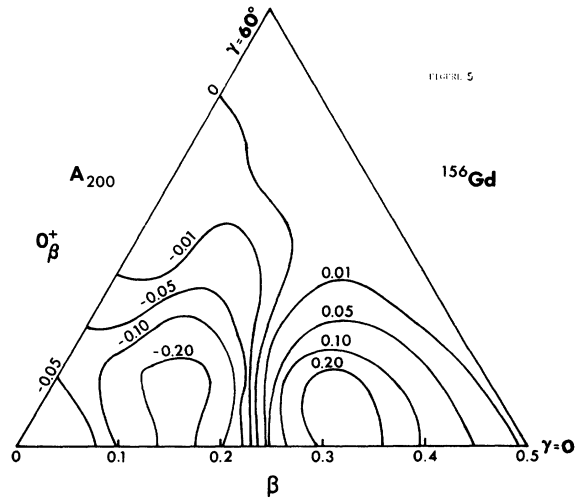

FIG. 5. Contour plot of the β-bandhead wave function of ^{156}Gd. As expected for a $n_\beta = 1$ wave function, there is a node near the potential minimum.

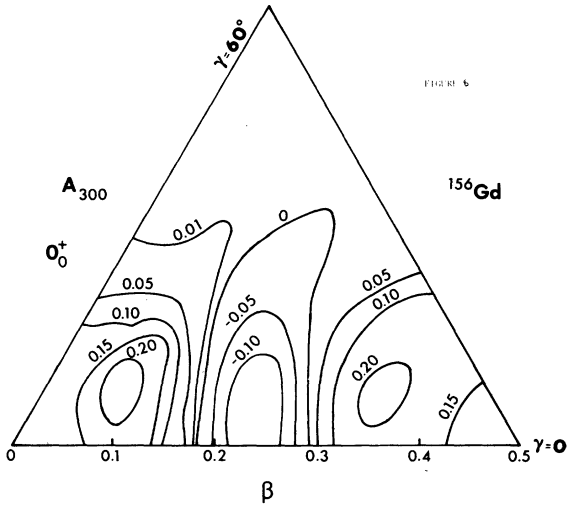

FIG. 6. Contour plot of the 0^+-bandhead wave function of ^{156}Gd. As expected for a $n_\beta = 2$ wave function, there are two nodes along the prolate edge.

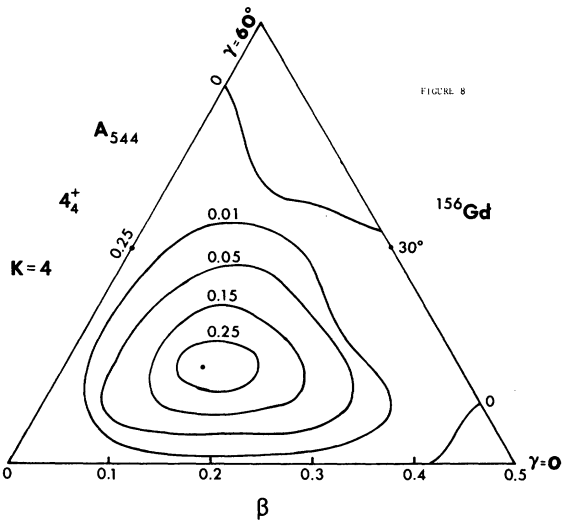

FIG. 8. Contour plot of the $K = 4$ component of the 4^+-bandhead wave function of ^{156}Gd. The $K = 2$ maximum, not shown here, is 20% of the maximum shown here.

and 5^+ states of the $K = 4$ band (see Fig. 8 for the bandhead). Note that the $K = 2$ maximum is only 20% of the $K = 4$ maximum of the $K = 4$ bandhead wave function.

F. $B(E2)$ values

1. Absolute $B(E2)$ values

Recent Coulomb excitation experiments of Hamilton *et al.*[5,14] give absolute $B(E2)$ values for excitation from the g.s. to 2_g and to three other 2^+ excited states. These are compared with the present theory in Table III. Riedinger, Johnson, and Hamilton[15] noted that the Coulomb excitation values of Yoshizawa *et al.*[16] for $B(E2; 0 \rightarrow 2_\gamma)$ in ^{152}Sm and ^{154}Gd needed correction for the β-γ bandmixing which would raise their values. A similar correction in ^{156}Gd raises their $B(E2; 0 \rightarrow 2_\gamma)$ from 0.06 to 0.12 and brings it in agreement with the value obtained by Hamilton *et al.*[14] This new value is in excellent agreement with our theory which takes into account the bandmixing.

The $B(E2)$ values for exciting the states 2_γ, 2_β, 2_0, and 4_4 are reduced[14,17,18] compared to the $B(E2; 0_g \rightarrow 2_g)$ value by 1, 2, 3, and 5 orders of magnitude, respectively. These order of magnitude reductions are reproduced remarkably well by the present theory (Table III).

Rud, Nielsen, and Wilsky[19] deduced the $B(E2; \beta \rightarrow g)$ values from their electron conversion measurements of $\mu_k(E0/E2)$, combined with the $B(E2; 0_g \rightarrow 2_g)$ values from Coulomb excitation.

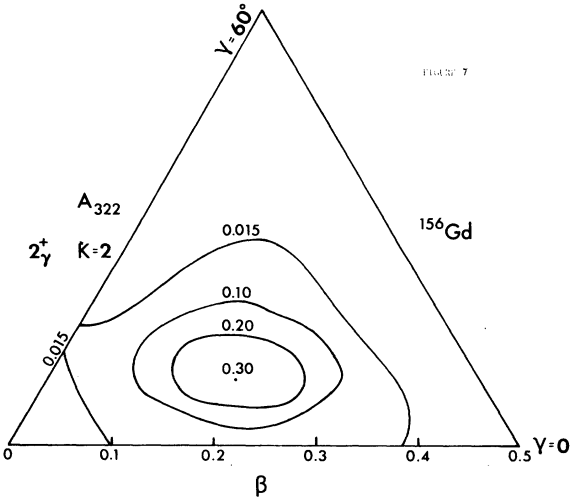

FIG. 7. Contour plot of the $K = 2$ component of the γ-bandhead wave function of ^{156}Gd. The $K = 0$ component, not shown here, contributes 14% to the normalization of the wave function.

TABLE II. Spectroscopic quadrupole and magnetic moments for ^{156}Gd.

	Expt.	Theo.
$Q(2_g)$ (e b)	-2.40 ± 0.25 [a]	-1.88
$\mu(2_g)$ (μ_N)	0.772 ± 0.008 [a]	0.82
$\mu(4_g)$ (μ_N)	1.48 ± 0.20 [b] 1.32 ± 0.36 [c]	1.63
$\mu(4_4)$ (μ_N)	3.12 ± 0.20 [b] 3.14 ± 0.40 [c]	1.6

[a] See Ref. 10.
[b] See Ref. 11.
[c] See Ref. 12.

TABLE III. Absolute $B(E2)$ values in e^2b^2 for ^{156}Gd.

Transition	Expt.	Theo.
$0_g \rightarrow 2_g$	4.57 ± 0.05 [a]	4.35
$0_g \rightarrow 2_\beta$	0.013 ± 0.004 [a]	0.020
$0_g \rightarrow 2_\gamma$	0.120 ± 0.004 [a]	0.143
$0_g \rightarrow 2_0$	<0.008 [a]	0.002
$2_g \rightarrow 4_4$	(1.6×10^{-5}) [b]	6.0×10^{-5}
$4_g \rightarrow 4_4$	(4.8×10^{-5}) [b]	2.6×10^{-5}
$2_g \rightarrow 4_g$	2.32 ± 0.04 [c]	2.30
$4_g \rightarrow 6_g$	2.13 ± 0.05 [c]	2.11

[a] See Ref. 14.
[b] See Ref. 17.
[c] See Ref. 18.

Their values along with the data from Coulomb excitation experiments[19,20] are compared with the present theory in Table IV. Calculated values for ^{154}Gd are taken from Ref. 21. For this nucleus, the agreement is good except for the $4_\beta \rightarrow 2_g$ transition. For ^{156}Gd, values from the present theory are generally larger.

2. *B(E2) branching ratios*

The $B(E2)$ branching ratios for the transitions from the β and γ vibrational bands to the g band in ^{156}Gd and ^{154}Gd are compared with experiment[15,22-27] in Table V. The agreement is reasonably good for ^{154}Gd except for the $4_\beta \rightarrow 2_g / 4_\beta \rightarrow 4_g$ ratio. There is fair agreement in ^{156}Gd for several transitions but there is substantial disagreement in others. Some of the $B(E2)$ values, e.g., those for the $4_\beta \rightarrow 4_g$ and $4_\beta \rightarrow 2_g$ transitions are quite sensitive to the renormalization parameters of the calculation. This problem will be discussed further in Sec. IV.

Table V also gives the $B(E2)$ branching ratios for transitions from the second 0^+ vibrational band to the g band for ^{156}Gd. Again, while the agreement with experiment is good for some transitions, it is quite bad for others.

The nature of an excited 0^+ state is often interpreted in terms of the ratio[28]

$$R = B(E2; 0'^+ \rightarrow 2_\gamma)/B(E2;\ 0'^+ \rightarrow 2g)\ . \qquad (8)$$

If the $0'^+$ state is interpreted as a β-vibrational state, then one gets $R = 0$. If the $0'^+$ state is interpreted as a 2γ phonon state, then $R = \infty$. The calculated $B(E2)$ values give $R(O_\beta) = 0.28$ and $R(O_0) = 17$, while the ratio $B(E2; 0_0 \rightarrow 2_\gamma)/B(E2; 0_0 \rightarrow 2_\beta)$ equals 0.44.

Unfortunately, the β, γ, and 0^+ bands are too close in energy to experimentally observe transitions between them. However, the calculated R values indicate that the main component of the calculated 0^+ bandhead is not 2γ photon in character. On the basis of large $M1$ components from a similar band in ^{152}Sm, a two quasiparticle state mixing is considered a possibility.[2] An explanation of this band in terms of a mixed prolate plus oblate plus spherical m band has been discussed previously in Sec. III E.

The $B(E2)$ branching ratios for transitions from the $K^\pi = 4^+$ band are given in Table VI. The experimental values[8,24,27] are compared with the present theory, as well as with the rotation-vibration model[1] (assuming the band to be a pure $K = 4$ band). The experimental values reported here have been corrected for the large $M1$ admixtures reported by Hamilton *et al.*[8] for the $5_4 \rightarrow 4_4$, $5_4 \rightarrow 5_\gamma$, $4_4 \rightarrow 4_\gamma$, and $4_4 \rightarrow 4_g$ transitions. They have not been corrected for the $M3$ admixtures reported by Uluer *et al.*[29] for some of these transitions. The $M3$ admixtures are less than 0.5%.

TABLE IV. $B(E2)$ values for β-band to g-band transitions in 10^{-2} e^2b^2 for ^{154,156}Gd.

Transition		^{156}Gd			^{154}Gd		
		Expt.			Expt.		
i	f	Rud			Rud	Riedinger	Theo.
β	g	*et al.* [a]	Hagemann [b]	Theo.	*et al.* [a]	*et al.* [c]	
0	2	2.9(4)	15	11.5	21(3)	23 (or 32) [d]	22.0
2	0	0.20(4)	0.20	0.40	0.48(4)	0.48	0.37
2	2	1.05(13)	1.22	3.20	4.0(2)	4.0	3.30
2	4	1.15(23)	1.29	6.79	11.9(8)	12.0	8.66
4	2	0.31(10)		0.15	0.35(8)		0.60
4	4	0.9(3)		4.1	3.0(6)		3.37
4	6	0.6(3)		5.1	11.9(25)		

[a] See Ref. 19. $B(E2)$ values obtained from $\mu_k(E0/E2)$ by assuming $\rho(E0) =$ constant and by taking $B(E2; 0_g \rightarrow 2_\beta)$ from Coulomb excitation (Refs. b and c).
[b] G. B. Hagemann, values tabulated in Ref. a.
[c] See Ref. 20.
[d] This depends on the choice of $E2$ matrix elements for $\beta \rightarrow \gamma$ transitions.

TABLE V. The $B(E2)$ branching ratios for ^{154,156}Gd.

I_i	I_f/I_f'	^{156}Gd Expt.[a]	^{156}Gd Theo.	^{154}Gd Expt.[b]	^{154}Gd Theo.
		β band $\rightarrow g$ band			
2	0/2	0.185±0.019	0.12	0.121±0.04	0.11
2	4/2	1.36±0.10	2.1	2.75±0.08	2.61
2	0/4	0.137±0.016	0.05	0.044±0.004	0.043
4	2/4	0.19±0.07[c]	0.04	0.086±0.003	0.18
4	6/4	3.4[c]	1.25	2.38±0.08[d]	
		0.65±0.26[e]			
4	2/6	0.05[c]	0.03		
		0.55±0.22[e]			
		γ band $\rightarrow g$ band			
2	0/2	0.67±0.03	0.64	0.458±0.010	0.56
2	4/2	0.086±0.017	0.20	0.144±0.005	0.089
2	0/4	7.9±1.6	3.22	3.2±0.4	6.3
3	2/4	1.52±0.08	1.38	0.984±0.026	0.70
4	2/4	0.152±0.013[c]	0.40	0.139±0.007	0.316
4	6/4	0.07[c]	0.66	0.27±0.04	
4	6/2	0.43[c]	1.6		
5	4/6	0.71±0.09[f]	0.82		
		1.35±0.15[e]			
2	$2_\beta/2_g$			1.0±0.02	1.47
		Second 0^+ band $\rightarrow g$ band			
2	0/2	0.223±0.025	0.44		
2	4/2	3.35±0.27	1.82		
2	0/4	0.070±0.007	0.24		
4	2/4	0.10±0.03[c]	1.2		
4	6/4	1.6±0.5	1.9		
4	2/6	0.06±0.02	0.6		

[a] Kluk *et al.*, Ref. 22, values based on coincidence work.

[b] Weighted average of the values measured by Riedinger *et al.* (Ref. 15) and by Meyer, Ref. 23.

[c] McMillán *et al.*, Ref. 24.

[d] The error in this ratio is corrected here as discussed in Ref. 25.

[e] Bäcklin *et al.*, (n,γ) work, Ref. 26.

[f] Siddiqi *et al.*, Ref. 27.

TABLE VI. $B(E2)$ branching ratios for transitions from the $K^\pi = 4^+$ band in ^{156}Gd. R-V denotes rotation-vibration model.

Transitions I_i	I_f/I_f'	E_γ (keV)	$B(E2)$ ratio Expt.[a]	Theo. (Present)	R-V Model[a,b]
4_4	$2_g/4_g$	1422/1222	0.23(1)[c]	1.3	0.34
	$6_g/2_g$	926/1422	2.72(14)		0.25
	$6_g/4_g$	926/1222	0.62(2)[c]		0.09
	$3_\gamma/2_\gamma$	263/357	2.03(13)	1.13	0.56
	$4_\gamma/2_\gamma$	155/357	1.46(25)[d]	0.41	
	$4_\gamma/3_\gamma$	155/263	0.71(14)[d]	0.36	
	$4_\beta/2_\beta$	213/381	0.24(40)[d]	0.59	
5_4	$3_\gamma/4_\gamma$	375/267	0.09(30)[d]	0.33	
			0.20(6)[e]		
	$3_\gamma/5_\gamma$	375/116	0.04(12)[d]	0.27	
	$4_\gamma/5_\gamma$	267/116	0.44(88)[d]	0.84	

[a] McMillan *et al.*, Ref. 24.

[b] Using relations given in Ref. 1 for a pure $K=4$ to $K=0$ transition.

[c] Taking the 1222 keV transition to be 81% $E2$, as determined from the internal-conversion coefficient experiment (Ref. 8).

[d] Values determined from the γ-ray intensity ratios. The 155, 116, and 213 keV transitions are taken to be 18.7%, 4.5%, and 19.4% $E2$, respectively, as determined from the internal-conversion coefficient experiment (Ref. 8).

[e] Using γ-ray intensity ratios from Ref. 27 for the 267 and 375 keV transitions, and assuming that the placement of the later transition is correct.

G. $E2, M1$ transition matrix elements

These matrix elements, especially their signs, are of interest for the analysis of Coulomb excitation data for $B(E2)$ values and quadrupole moments, and of the directional correlation experiments for the mixing ratios $\delta(E2/M1)$.

These matrix elements are obtained in the present theory by first calculating the expectation values of the appropriate operators in a microscopic (deformed-quasiparticle) basis and then averaging the expectation values over all relevant shapes of the nucleus. Details of the method of calculation can be found in Ref. 7. For the reader's convenience, we note that

$$M_{sr}(\lambda) = (-1)^{I_r - I_s} M_{rs}(\lambda) \tag{9}$$

and

$$B(\lambda; r \rightarrow s) = (2I_r + 1)^{-1} M_{rs}^2(\lambda) \ . \tag{10}$$

Only the nondiagonal matrix elements are given in Tables VII and VIII since the diagonal matrix elements can be deduced from the quadrupole and magnetic moments given in Table I via[7]

$$Q^S(I) = -\{16\pi I(2I-1)/[5(I+1)(2I+1)(2I+3)]\}^{1/2} M_{II}(E2) \ , \tag{11}$$

$$\mu^S(I) = \{4\pi I/[3(I+1)(2I+1)]\}^{1/2} M_{II}(M1) \ . \tag{12}$$

TABLE VII. Calculated $E2$ matrix elements between states of spin I_r and I_s in the different bands in ^{156}Gd, $M_{rs}(E2) = \langle s \| i^2 \mathfrak{M}(E2) \| r \rangle$ in e b.

I_r	I_s	$g \rightarrow g$	$\beta \rightarrow \beta$	$\gamma \rightarrow \gamma$	$0^+ \rightarrow 0^+$		
2	0	−2.09	−2.03		−1.91		
4	2	−3.39	−3.38	−2.10	−3.00		
6	4	−4.35					
3	2			3.17			
4	3			2.93			
5	3			−2.97			
5	4			2.86			
I_r	I_s	$\beta \rightarrow g$	$0^+ \rightarrow g$	$0^+ \rightarrow \beta$	$\gamma \rightarrow g$	$\gamma \rightarrow \beta$	$0^+ \rightarrow \gamma$
0	2	−0.34	−0.04	0.77			0.16
2	4	−0.58	−0.10	0.85	−0.21	0.12	−0.38
2	2	0.40	0.07	−0.60	−0.47	0.93	−0.05
2	0	−0.14	−0.05	0.16	−0.38	−0.18	
3	4				−0.47	1.06	
3	2				−0.55	−0.28	
2	3						−0.14
4	3						0.17
4	6	−0.68	−0.10		−0.46		
4	4	0.61	0.07	−0.94	−0.57	−0.79	−0.06
4	2	−0.11	−0.08	0.38	−0.36	0.57	0.004
5	6				−0.66		
5	4				−0.60		
4	5						0.44

1. *E2 matrix elements*

These are given in Table VII. Note that within a rotational band, the matrix elements for intraband transitions are of approximately the same magnitude. In addition to the major K components of the wave functions mentioned above, we have employed this constancy of $E2$ matrix elements in grouping the various states into rotational bands built on different intrinsic or vibrational states.

The interband transition matrix elements are in general smaller by an order of magnitude. Thus, the corresponding $B(E2)$ values are smaller by two orders of magnitude. All this agrees with the rotational model of Bohr and Mottelson.[1] However, note that the matrix elements connecting the γ and β bands are just as large, or even larger [the calculated $3_\gamma \rightarrow 4_\beta$ matrix element is the largest interband matrix element (m.e.) in the table], as those connecting γ and g or β and g. Such large γ and β matrix elements have not been measured in ^{156}Gd yet, but they have been measured for ^{154}Sm (see the discussion in Ref. 4). These matrix elements give us the warning that even in a nucleus like ^{156}Gd, which is quite deformed, our grouping of nuclear states into g, β, γ, ... bands should not be taken too seriously.

The $E2$ matrix elements for the decay of the 0^+ band shed some interesting light on the nature of this band. While the $0^+ \rightarrow g$ theoretical matrix elements are small compared to either $\beta \rightarrow g$ or $\gamma \rightarrow g$, as we might expect for a $\Delta n_\beta = 2$ or a $\Delta n_\gamma = 2$ transition, most of the $0^+ \rightarrow \beta$ and $0^+ \rightarrow \gamma$ m.e. are large compared to $0^+ \rightarrow g$ by a factor of 2 or more. Since the $0^+ \rightarrow \beta$ ones are larger, we may call the 0^+ band an $n_\beta = 2$ band with substantial mixing of $n_\gamma = 2$ phonons. Again we note the experimental second 0^+ band may not be the second 0^+ band we have calculated.

A detailed comparison of the magnitudes and signs of our calculated $E2$ matrix elements with those needed for Coulomb excitation analysis has recently been made by Ronningen *et al.*[14] A remarkable agreement is obtained.

2. *M1 matrix elements*

These are given in Table VIII. The calculated $M1$ matrix elements for $\gamma \rightarrow g$ transitions are somewhat weaker than those for $\beta \rightarrow g$ transitions. Note that as in the case of the $E2$ m.e., the $M1$ m.e. for $\gamma \rightarrow \beta$ transitions are substantial. Matrix elements for the $\gamma \rightarrow \gamma$ transitions are of the same order as $\beta \rightarrow g$ and $\gamma \rightarrow g$. Such $\gamma \rightarrow \beta$ and $\gamma \rightarrow \gamma$ m.e. are forbidden in the first order band-mixing theory (see, e.g., Ref. 7). However, it must be noted that all the $M1$ transition matrix elements are reduced compared to the diagonal $M1$ m.e. [which may be deduced from Table I and Eq. (12)] by two or more orders of magnitude (note the factor of 10^{-2} in the units in Table VIII).

The $M1$ transition matrix elements for the decay of the 0^+ band show some interesting features. Those for $0^+ \rightarrow g$ are of the same order as $\beta \rightarrow g$ or $\gamma \rightarrow g$. Those for $0^+ \rightarrow \beta$ are larger than either $\beta \rightarrow g$ or $\gamma \rightarrow g$. These matrix elements suggest that members of the 0^+ band involve mixing of not only 2β and 2γ phonons (as deduced from $E2$ matrix elements) but also of many other β and γ phonons.

3. *Mixing ratios δ(E2/M1)*

The mixing ratio is defined as[30]

$$\delta(E2/M1) = [\Gamma(E2)/\Gamma(M1)]^{1/2} = -0.835(E_\gamma \text{ in MeV}) \times [M_{rs}(E2) \text{ in } e\,\text{b}]/[M_{rs}(M1) \text{ in } \mu_N] , \quad (13)$$

where $\Gamma(E2)$ is the γ-ray decay width for $E2$ transitions. Some of our calculated values (taking E_γ from experiment) are given in Table IX. Others can be obtained by combining Eq. (13) with the $E2$ and $M1$ matrix elements of Tables VII and VIII. Comparison with the experimental values[5,31] given in Table IX shows that the calculated values are in

TABLE VIII. Calculated $M1$ matrix elements for ^{156}Gd, $M_{rs}(M1) = \langle s \| \mathfrak{M}(M1) \| r \rangle$ in 10^{-2} μ_N.

I_r	I_s	$\gamma \to g$	$\beta \to g$	$0^+ \to g$	$\gamma \to \beta$	$0^+ \to \beta$	$\gamma \to 0^+$	$\gamma \to \gamma$
2	2	−1.02	−1.67	1.76	0.28	5.32	−0.09	
4	4	3.73	−4.52	3.59	3.45	12.15	−2.95	
3	2	−0.93			−0.57		0.78	−3.11
3	4	−1.01			1.27		0.29	3.85
5	4	−1.94			−1.23		1.82	4.90
5	6	−2.27						

general too large. As regards the sign, two of the values agree in sign while two disagree. Nothing is known about the systematics of the δ value for $2_0 \to 2_g$ transitions, but the experimental sign for $\delta(E2/M1; 2_\beta \to 2_g)$ disagrees with the systematics for all other nuclei of the region. This systematics[31] (for 13 cases) shows that the signs of δ values are opposite for $\beta \to g$ and $\gamma \to g$ transitions.

In any case, it is clear that the agreement of theoretical and experimental δ values for ^{156}Gd is not as good at all as that obtained previously for the Os region[7,30] and the Sm region.[4] This problem is discussed further in Sec. IV. Table IX also shows that in terms of the % $E2$ transition probability, the main discrepancy in the calculated values occurs for the $2_0 \to 2_g$ transition.

IV. SUMMARY AND CONCLUSIONS

The pairing-plus-quadrupole model of Kumar and Baranger[3,4,7] is used for calculating microscopically the collective spectrum of ^{156}Gd. Discussion is given of the general features of the potential energy of deformation, rotational moments of inertia, vibrational mass parameters, energy levels, and electromagnetic moments of ^{156}Gd. Some results from a similar calculation for ^{154}Gd are also given. We summarize below the main results and conclusions of this study.

1. Energy level spacings for the g, β, γ, 0^+, and 4^+ bands are reproduced well. However, the calculated β, γ, 0^+, and 4^+ bandheads are shifted upwards by 0.2, 0.4, 1.1, and 1.5 MeV, respectively.
2. The spectroscopic quadrupole moment of the first 2^+ state and the magnetic moments of the first 2^+ and 4^+ states are reproduced well.
3. The present calculation reproduces remarkably well the absolute $B(E2)$ values for the excitation of various bandheads, although the experimental values for the different bands vary by five orders of magnitude.
4. Agreement with the $B(E2)$ values for interband transitions not involving the ground state is in general not so good.
5. The calculated $\delta(E2/M1)$ values agree with the sign of the experimental values in two cases but disagree in two other cases. The calculated magnitudes are too large by factors ranging from 2 to 10.

Our main conclusion is that the dynamic, microscopic method of Kumar and Baranger can be used for well-deformed nuclei. We know of no other available method which provides such a wealth of predictions with so few parameters.

Discrepancies with the $B(E2)$ values and the $E2/M1$ mixing ratios noted above, and the study of the two renormalization parameters of the theory, suggest that the main problem with the present theory lies with the shell model type of division of the nucleus into an inert core and a cloud of valence nucleons. Recently[32] the dynamic theory of Kumar and Baranger has been combined with the Nilsson Model, as modified by Strutinsky, where a complete configuration space is employed and the renormalization parameters are removed.

One of us (J.B.G.) is thankful to Professor L. S. Kothari for his encouragement and for the use of facilities at the University of Delhi.

TABLE IX. Theoretical and experimental $E2$ and $M1$ mixing ratios for ^{156}Gd.

Transition	E_γ (MeV)	$\delta(E2/M1)$ Theo.	$\delta(E2/M1)$ Expt.	% $E2$ Theo.	% $E2$ Expt.
$2_\beta \to 2_g$	1.040	20.8	$-5.9^{+1.4}_{-2.8}$ [a]	99.8	$97.2^{+1.5}_{-1.9}$
$4_\beta \to 4_g$	1.010	11.3		99.2	
$2_\gamma \to 2_g$	1.065	−41.0	-18 ± 3 [a]	99.9	99.7(1)
$3_\gamma \to 2_g$	1.159	−57.5	-10.0 ± 0.6 [b]	100.0	99.0(1)
$3_\gamma \to 4_g$	0.960	−37.3		99.9	
$4_\gamma \to 4_g$	1.067	13.7	c	99.5	
$2_0 \to 2_g$	1.169	−3.9	$0.38^{+0.06}_{-0.05}$ [a]	93.8	$12.6^{+4.6}_{-2.8}$
$4_0 \to 4_g$	1.174	−1.9		78.3	

[a] Hamilton *et al.*, Ref. 5.
[b] Hamilton (unpublished) and Ref. 31.
[c] Uluer *et al.*, Ref. 29, report this transition to be predominantly $E2$.

†Work supported partially by U. S. Energy Research and Development Administration.

[1]A. Bohr and B. R. Mottelson, K. Dan. Vidensk. Selsk. Mat.-Fys. Medd. 27, No. 16 (1953); *Nuclear Structure* (Benjamin, New York, 1975).

[2]J. H. Hamilton, Izv. Akad. Nauk. SSSR Ser. Fiz. 36, 17 (1972) [Bull. Acad. Sci. USSR Phys. Ser 36, 17 (1972)].

[3]K. Kumar and M. Baranger, Nucl. Phys. A122, 273 (1968).

[4]K. Kumar, Phys. Rev. Lett. 26, 269 (1971); Nucl. Phys. A231, 189 (1974).

[5]J. H. Hamilton *et al.*, in *Proceedings of the International Conference on Nuclear Physics, Munich*, 1973, edited by J. de Boer and J. H. Mang (North-Holland, Amsterdam/American Elsevier, New York, 1973), Vol. 1, p. 294; W. E. Collins *et al.*, Phys. Rev. C (to be published).

[6]J. B. Gupta, J. H. Hamilton, and K. Kumar, in *Proceedings of the International Conference on Nuclear Physics, Munich*, 1973 (see Ref. 5), p. 157.

[7]K. Kumar, in *The Electromagnetic Interaction in Nuclear Spectroscopy*, edited by W. D. Hamilton (North-Holland, Amsterdam, 1975), Chap. 3, p. 55.

[8]J. H. Hamilton, M. Fujioka, J. J. Pinajian, and D. J. McMillan, Phys. Rev. C 5, 1800 (1972).

[9]A. F. Kluk, N. R. Johnson, and J. H. Hamilton, Phys. Rev. C 10, 1451 (1974).

[10]H. Armon *et al.*, Nucl. Phys. A233, 385 (1974).

[11]A. Weitsch and H. K. Walter, in *Hyperfine Structure and Nuclear Radiations*, edited by E. Matthias and D. A. Shirley (North-Holland, Amsterdam, 1968), p. 167.

[12]S. N. Khan, R. A. Fox, W. D. Hamilton, and M. Finger, J. Phys. G 1, 727 (1975).

[13]K. Kumar and M. Baranger, Nucl. Phys. A92, 608 (1967); K. Kumar, *ibid.*, A92, 653 (1967).

[14]J. H. Hamilton, A. V. Ramayya, L. L. Riedinger, P. H. Stelson, and R. L. Robinson, Bull. Am. Phys. Soc. 18, 655 (1973); R. M. Ronningen *et al.*, Phys. Rev. C 15, 1671 (1977).

[15]L. L. Riedinger, N. R. Johnson, and J. H. Hamilton, Phys. Rev. 179, 1214 (1969).

[16]Y. Yoshizawa, B. Elbek, B. Herskind, and M. C. Olesen, Nucl. Phys. 73, 273 (1965).

[17]W. Andrejtscheff *et al.*, At. Data Nucl. Data Tables 16, 515 (1975).

[18]D. Ward, R. L. Graham, G. S. Geiger, N. Rud, and A. Christy, Nucl. Phys. A196, 9 (1972).

[19]N. Rud, H. L. Nielsen, and W. Wilsky, Nucl. Phys. A167, 401 (1971).

[20]L. L. Riedinger *et al.*, in *Proceedings of the International Conference on Nuclear Reactions Induced by Heavy Ions, Heidelberg*, edited by R. Bock and W. R. Hering (North-Holland, Amsterdam, 1969), p. 442.

[21]J. B. Gupta, Ph.D thesis, Vanderbilt University, Nashville, 1973 (unpublished); J. B. Gupta, K. Kumar, and J. H. Hamilton (unpublished).

[22]A. F. Kluk, N. R. Johnson, and J. H. Hamilton, Z. Phys. 253, 1 (1972).

[23]R. A. Meyer, Phys. Rev. 170, 1089 (1968).

[24]D. J. McMillan, J. H. Hamilton, and J. J. Pinajian, Phys. Rev. C 4, 542 (1971).

[25]J. B. Gupta *et al.*, Z. Phys. (to be published).

[26]A. Bäcklin *et al.*, in *Neutron Capture γ-ray Spectroscopy* (IAEA, Vienna, 1969), p. 147.

[27]T. A. Siddiqi, F. P. Cranston, and D. H. White, Nucl. Phys. A179, 609 (1972).

[28]M. R. McPhail, R. F. Casten, and W. R. Kane, Phys. Lett. 59B, 435 (1975).

[29]I. Uluer *et al.*, J. Phys. G 1, 476 (1975).

[30]K. Kumar, Phys. Lett. 29B, 25 (1969).

[31]W. D. Hamilton and K. Kumar (unpublished).

[32]K. Kumar, B. Remaud, P. Auger, J. S. Vaagen, A. C. Rester, R. Foucher, and J. H. Hamilton, Phys. Rev. C (to be published).